Calculation of irradiance distribution on PV modules by combining sky and sensitivity maps

Santbergen, R.; Muthukumar, V.A.; Valckenborg, R.M.E.; van de Wall, W.J.A.; Smets, A.H.M.; Zeman, M.

DOI
10.1016/j.solener.2017.04.036

Publication date
2017

Document Version
Accepted author manuscript

Published in
Solar Energy

Calculation of irradiance distribution on PV modules by combining sky and sensitivity maps

R. Santbergen[a,*], V.A. Muthukumar[a,b], R.M.E. Valckenborg[b], W.J.A. van de Wall[c], A.H.M. Smets[a], M. Zeman[a]

[a] *Photovoltaic Materials and Devices, Delft University of Technology, Mekelweg 4, 2628 CD, Delft, the Netherlands*
[b] *Solar Energy Application Centre (SEAC), High Tech Campus 21, 5656 AE, Eindhoven, the Netherlands*
[c] *Wallvision B.V, Deken de Bruijnplein 3, 5591 CZ Heeze, the Netherlands*

Abstract

Photovoltaic (PV) modules receive both direct light from the sun and scattered light from the sky, ground and nearby objects. The calculation of incident irradiance becomes complex when nearby objects cast shadows or reflect sunlight onto the PV modules. In this paper a flexible irradiance model is presented that takes all these effects into account by combining a so-called sky map, obtained from the Perez model, with a sensitivity map, generated using a ray tracing software. This irradiation model is validated for a PV facade that combines PV modules with mirror reflectors and is shown to be a flexible tool to accurately predict the irradiance distribution.

1. Introduction

When designing a photovoltaic (PV) system it is important to predict the annual energy yield for a given location. Being able to predict the power output for each of the design options allows one to select the optimum design. Software packages like PVsyst[1] are commonly used for this. Internally such software packages use an irradiance model to predict the irradiance incident on the PV modules. Input for such an irradiance model are typically the measured hourly values of direct normal irradiance (DNI) and diffuse horizontal irradiance (DHI), for example from the Meteonorm database[2]. From this, the hourly irradiance on the PV module is calculated taking into account its orientation and tilt.

For conventional flat PV modules that are not exposed to shading or reflection from nearby structures, accurate irradiance models exist. These models usually calculate the direct irradiance from the DNI and sun position, while diffuse irradiance is calculated using one of the tilted surface models[3]. Also the albedo of the ground is usually included. However, in some PV systems, reflective surfaces are included to increase the power output of the PV system. One example of such a system is the patented ZigZagSolar^{TM} building integrated photovoltaic (BIPV) facade indicated in Fig. 1. In this system a facade is covered with alternating rows of PV modules and reflectors, each placed at a specific angle with the aim to combine an aesthetic appearance with a high annual energy yield. For PV systems like this, the conventional irradiance models cannot accurately predict the additional irradiance on the PV module due to the reflector, taking into account the sun position, reflector angle and PV module angle. Irradiance models for this type of PV system have been developed[4], but these are not generally applicable to a wide range of PV systems. In this paper a more flexible and general approach is proposed that can be used for any type of PV system. The proposed irradiance model can calculate the solar irradiance distribution on any surface such as PV module or solar thermal collector, even when it has a complex geometry, is partly shaded, receives irradiance from reflectors or when a concentrator lens or mirror is used to focus light onto the surface.

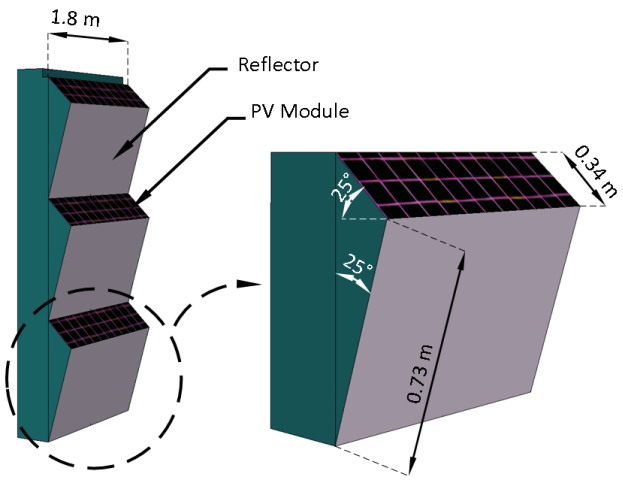

Figure 1: Schematic of the ZigZagSolar^{TM} BIPV facade.

The irradiance model has some similarities with the model developed by Kolås et al.[5] and with daylight simulations for indoor building environments based on the concept of daylight coefficients[6]. Several software packages based on

*Corresponding author
Email address: r.santbergen@tudelft.nl (R. Santbergen)

that approach are available such as DDS standard model[7] and Daysim daylight coefficient model[8]. However, it will be shown here that a similar approach can also be used for simulating the irradiance on outdoor surfaces, such as PV modules. The objective of this paper is to show that this results in a novel, flexible and accurate irradiance model that can aid in the prediction of the annual yield of PV systems.

2. Model description

The irradiance model calculates the irradiance incident on a PV module by combining a so-called sky map, characterizing the irradiance conditions, with a sensitivity map, characterizing the geometry and optical properties of the PV system and its surroundings. This will be explained in more detail below.

2.1. Calculation of sky map

The Perez model takes the easily measurable DNI and DHI values and from that reconstructs the luminance distribution of the circumsolar and diffuse light across the sky[9]. This luminance distribution combined with the direct irradiance component will be called the sky map. Fig. 2 and Fig. 3 show the sky maps for one instant in time. The centre of the figure indicates the zenith position and the edge represents the horizon, with North, East, South and West indicated. Fig. 2 represents a sunny instant in time and the obvious bright spot indicates the sun position surrounded by the circumsolar light. Away from the sun position the sky is less bright and more subtle variations in sky luminance can be observed. Fig. 3 shows the sky map for an overcast instant in time and under these conditions no bright spot is visible.

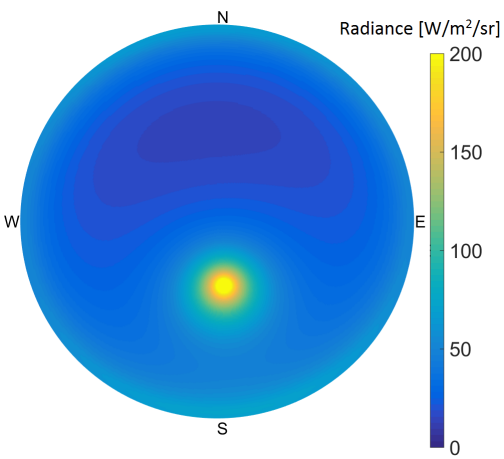

Figure 2: Sky map for a sunny instant in time (with DNI = 905 W/m^2 and DHI = 111 W/m^2) .

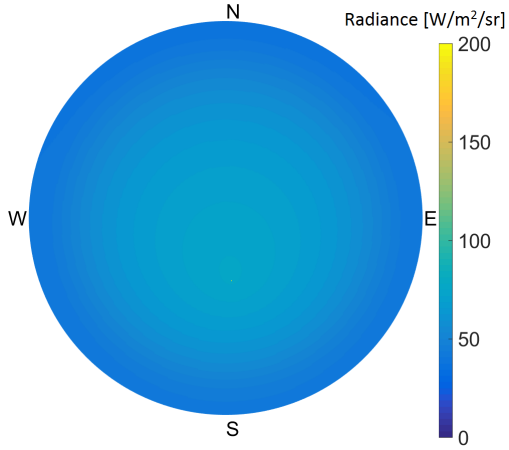

Figure 3: Sky map for an overcast instant in time (with DNI = 1 W/m^2 and DHI = 198 W/m^2).

Since hourly data for the DNI, DHI and sun position are available for many locations for a full year, this information can be used to create a sky map for each hour of the year. It is then possible to integrate the sky map over the entire year, resulting in a so-called integral sky map. As an example, Fig. 4 shows the integral sky map for the city of Eindhoven in the Netherlands (51°26N 5°29E). Because it is based on hourly data, the hourly analemma are visible.

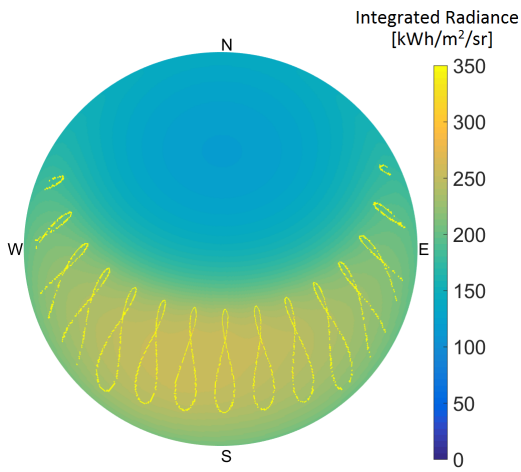

Figure 4: Integral sky map for entire year based on hourly meteorological data from the city of Eindhoven, Netherlands (51°26N 5°29E).

2.2. Calculation of sensitivity map

A sensitivity map contains a surface's sensitivity to incident light as a function of the hemispherical angle of incidence. This concept is illustrated for the ZigZagSolar^{TM} BIPV facade. A three-dimensional model of the ZigZagSolar^{TM} BIPV facade is constructed in the ray-tracing software LightTools[10], as shown in Fig. 5. The optical properties of each surface can be given as input. The reflector is assumed to be a mirror (reflecting

specularly) with a reflectance of 85 % and the PV cells are assumed to be prefect absorbers. To determine a PV cell's sensitivity for light from one particular direction, a ray tracing simulation is performed in which the whole object is illuminated from this direction and all possible reflections are taken into account. The software is based on the Monte-Carlo ray tracing approach. The incident light beam consists of parallel rays, as shown in Fig. 5, and has a fixed direct normal intensity I_{dn}. The path of each ray is traced until its energy is absorbed or it escapes to infinity. The tracing depth is set sufficiently high to assure that no rays are terminated. The output of this simulation is the power *absorbed* in each cell per unit cell area I_{abs}. The sensitivity S of a cell is then defined as

$$S = \frac{I_{\mathrm{abs}}}{I_{\mathrm{dn}}}. \tag{1}$$

For example, for a horizontal perfectly absorbing surface the sensitivity is given by $S = \cos\theta$ where θ is the zenith angle. This means that S varies between 0 for light incident from the horizon and 1 for light incident from zenith. Note that S can exceed 1 when light is concentrated, e.g. by a lens or mirror.

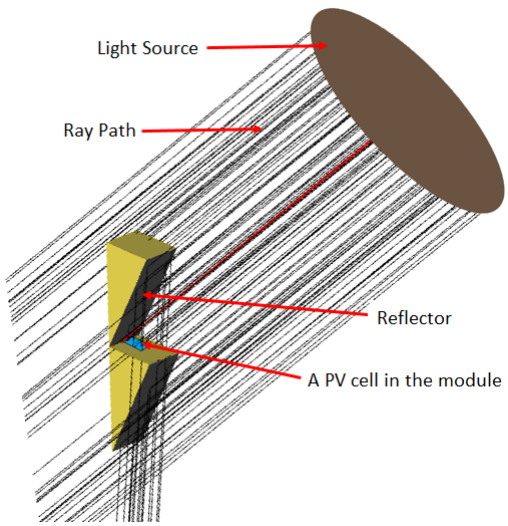

Figure 5: Ray tracing simulation of the ZigZagSolar^{TM} BIPV facade illuminated by a collimated beam incident from one particular direction.

The sensitivity of a surface can be mapped as a function of the hemispherical angle of incidence, resulting in the so-called sensitivity map. In this work an angular resolution of 10° is used, which means that 370 ray tracing simulations are required to obtain the full sensitivity map. For each ray tracing simulation 2.5 million incident rays are traced. Using a regular desktop computer, it takes about 1 hour to perform all 370 ray tracing simulations. Note that the sensitivity maps of all cells can be obtained from

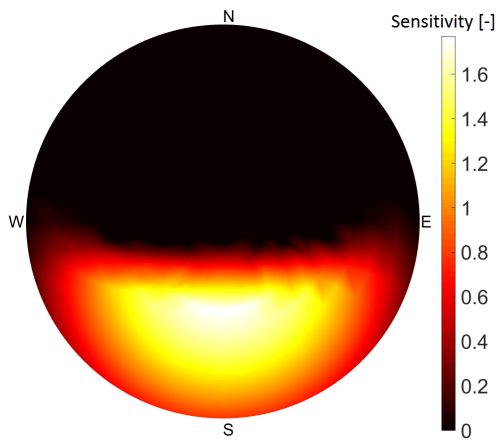

Figure 6: Sensitivity map for cell number 1.6 in the PV module based on ray tracing simulations for 370 different angles of incidence.

these simulations simultaneously. Fig. 6 shows the resulting sensitivity map of one PV cell in the ZigZagSolar^{TM} BIPV facade. This shows that a maximum sensitivity of 1.8 is reached for light incident from the South and elevation of around 50°. In this case the sensitivity exceeds 1, because the cell receives additional light from the mirror reflector. It is also obvious that this cell is insensitive ($S = 0$) for light incident from the North, as for that incident direction it is completely shaded.

Note that every cell in the PV module has a slightly different sensitivity map. When the design of the PV system is changed, for example using a different reflector angle, new ray tracing simulations are required to recalculate the sensitivity map. However, such recalculation is not required when the orientation of the system is changed, for example from South to West. In that case the sensitivity map can simply be rotated clockwise by 90° without requiring any recalculation.

2.3. Calculation of incident irradiance

The sky map contains the information on how much light is incident from each direction. The sensitivity map indicates the sensitivity of a surface for light from each direction. The total irradiance on a surface can then be calculated by integrating the product of the sky and sensitivity maps over the whole sky as given by Eq. (2).

$$Irradiance = \int_{sky} sky\,map \times sensitivity\,map \; \mathrm{d}\Omega. \tag{2}$$

By integrating the sensitivity map of each PV cell in the module over the same sky map, the irradiance distribution over all PV cells in the module is obtained. By repeating this for the hourly sky maps, the time evolution of this distribution is obtained. Alternatively a year integral sky map can be used, which directly gives the total yearly insolation.

Figure 7: Photo of ZigZagSolar^{TM} BIPV test setup.

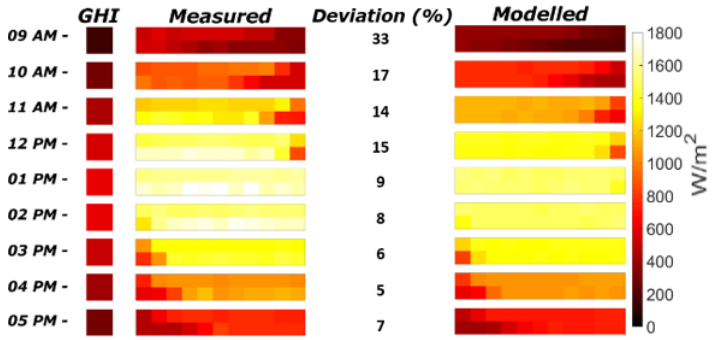

Figure 8: Comparison of the measured and modelled irradiance distribution on the PV module for every hour from 9 AM to 5 PM. The hourly GHI and the deviation between measurement and model are indicated as well.

3. Validation

The irradiance model described in the previous section was validated experimentally. For this, the irradiance distribution on the PV module of a ZigZagSolar^{TM} BIPV system was measured during one day and compared to simulation results.

3.1. Experimental setup

The experimental setup provided by ZigZagSolar^{TM}[11] is shown in Fig. 7. The reflector is a mirror, tilted 25° from the vertical. The PV module contains two rows of 11 mono c-Si PV cells and is tilted 25° from the horizontal. The setup is located near Eindhoven in Netherlands (51°26N 5°29E) and is oriented towards South direction. The measurements were performed on a sunny day with mostly clear skies. The incident irradiance on each of the 22 cells was measured every hour using a secondary standard pyranometer (MS-810 from EKO Instruments) with a sensitivity of 6.79 µV/Wm^{-2}.

3.2. Irradiance model setup

Next the measurement conditions are simulated in the irradiance model. The ZigZagSolar^{TM} BIPV system is created in the ray tracing software, with the same design as specified above. The reflector surface was given a fully specular reflectance of 85 %. The method described in section 2.2 was used to generate the sensitivity map for each of the solar cells in the PV module. The hourly sky maps are generated as described in section 2.1, using the weather data obtained from a nearby weather measuring station[12] for the day of the measurement. By combining these sensitivity maps and sky maps, as described in section 2.3, the incident irradiance on each of the 22 PV cells was obtained for every hour.

3.3. Comparison between measurement and modelled irradiance distribution

Fig. 8 shows a comparison between the measured and modelled irradiance distributions for every hour from 9 AM to 5 PM. The global horizontal irradiance (GHI) measured by the weather station, shown on the left side, reveals that the highest irradiance of about 700 W/m^2 is obtained at 1 PM. The measurement shows that the average irradiance on the PV module reaches its highest value at 1 PM as well. Due to the reflection from the mirror, the irradiance on the PV module is more than two times higher than the GHI. Closer inspection reveals that the irradiance on the PV module varies from cell to cell. For example, at 9 AM, the right side of the PV module is darker than its left side, while at 5 PM it is the other way round. Looking at the corresponding modelled result, it can be observed that it shows a good agreement with the measurement result. Even the darker areas that appear on the right side at 9 AM and on the left side at 5 PM are reproduced. The deviation between the measured and modelled irradiance is calculated for every PV cell. For every hour the average deviation of the 22 PV cells is shown in the same figure. It can be observed that in the morning the deviation was rather large, which is attributed to the presence of morning dew during the measurement, not included in the model. However, in the afternoon the deviation was less than 10 % indicating a very good agreement between measurement and model. From this it can be concluded that the irradiance model described in section 2 is accurate and is a valid tool for calculation of the incident irradiance. Note that the standard textbook irradiance model [13], used in most simulation software, deviates from the measured irradiance by as much 45 %. This is because the textbook model cannot take reflections from the mirror into account. Also note that the deviations presented here are specific for this ZigZagSolar^{TM} BIPV facade under sunny weather conditions. Further validation of the irradiance model for a wider range of weather conditions and BIPV systems will be presented in a future study.

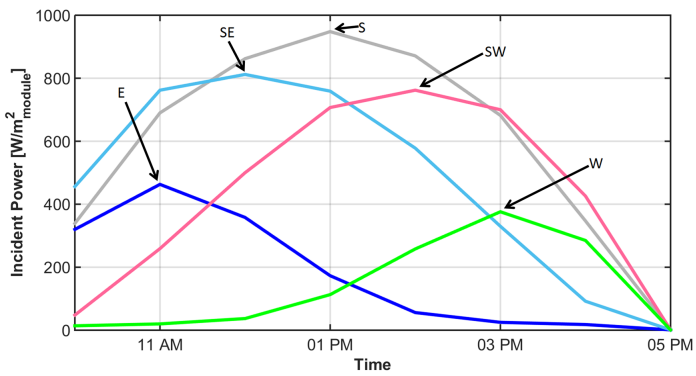

Figure 9: Simulated incident irradiance on the PV module during a sunny winter day in Eindhoven for different ZigZagSolar^{TM} BIPV facade orientations.

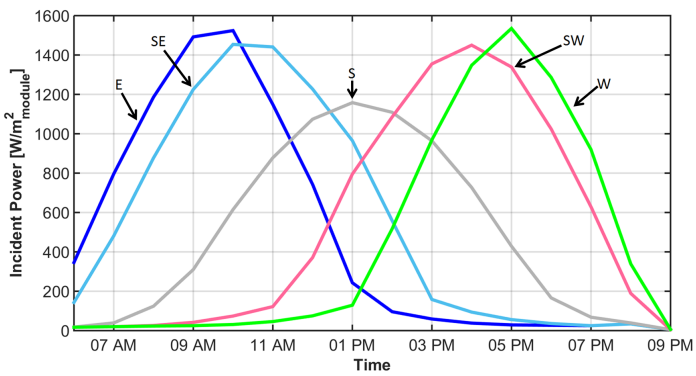

Figure 10: Simulated incident irradiance on the PV module during a sunny summer day in Eindhoven for different ZigZagSolar^{TM} BIPV facade orientations.

4. Results

To further illustrate the flexibility of the irradiance model, a ZigZagSolar^{TM} BIPV system is simulated for a sunny winter day and a sunny summer day, for different facade orientations (East, Southeast, South, Southwest and West). The sensitivity map of the ZigZagSolar^{TM} BIPV system is calculated with perfect mirror reflector and both reflector and PV angle of 25°. The facade orientation is varied by simply rotating the sensitivity maps. To generate the sky maps the weather data from the Meteonorm software[2] for the city of Eindhoven is used.

4.1. Sunny winter day

First the incident irradiance distribution on the PV module of the ZigZagSolar^{TM} BIPV geometry was simulated for a sunny winter day. Fig. 9 shows the irradiance averaged over 22 PV cells during this day, where each line represents a different facade orientation. As expected, the irradiance evolves differently for the different orientations. It can be seen that the peak irradiances occur at 11 AM, 12 PM, 1 PM, 2 PM and 3 PM for the East, Southeast, South, Southwest and West orientations respectively. The South oriented system receives the highest peak irradiance on its PV module surface, whereas the East and West facing system receive the lowest values.

4.2. Sunny summer day

The simulation was repeated for a sunny summer day. The same sensitivity maps are used as before but the sky maps are now calculated from the weather data and sun position of a sunny summer day. The resulting irradiance distributions are therefore different, as shown in Fig. 10. Surprisingly, the South facing system now has the lowest peak irradiance. This is attributed to the mirror reflector receiving less sunlight when the sun is at a large elevation. The systems with (South)East or (South)West orientation face the sun earlier in the morning or later in the afternoon, when the sun has a lower elevation. In that case the reflector receives more sunlight and reflects more light onto the PV module. This more than compensates for the somewhat lower GHI during these times.

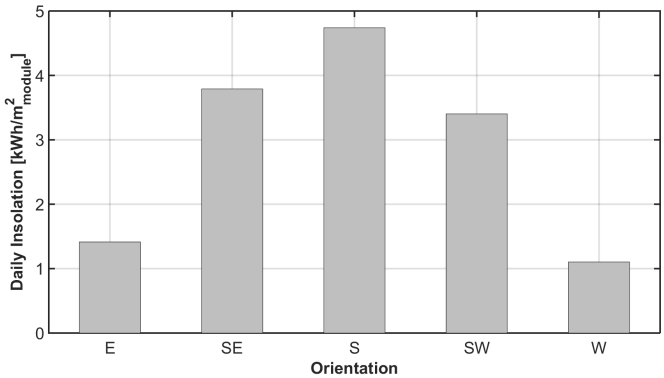

Figure 11: Daily insolation on the PV module of ZigZagSolar^{TM} BIPV facade in Eindhoven on a winter day as a function of facade orientation.

Additionally the *daily total* insolation on the PV module for the different orientations are shown in Fig. 11 for the winter day and in Fig. 12 for the summer day. They show that for a winter day the highest insolation on the PV module is achieved by the South oriented system, while for a summer day the South oriented system is outperformed by more than 10% by a Southeast or Southwest oriented system.

4.3. Full year simulation

To determine the annual insolation, one could calculate the irradiance on the PV module for every hour of the year and then take the sum. However, an advantage of this irradiance model based on Eq. (2) is that it can calculate the annual insolation in one step. This is done by using the integral sky map (for a full year, as shown in Fig. 4) as input. The simulation was done for the different orientations and the results are shown in Fig. 13. This

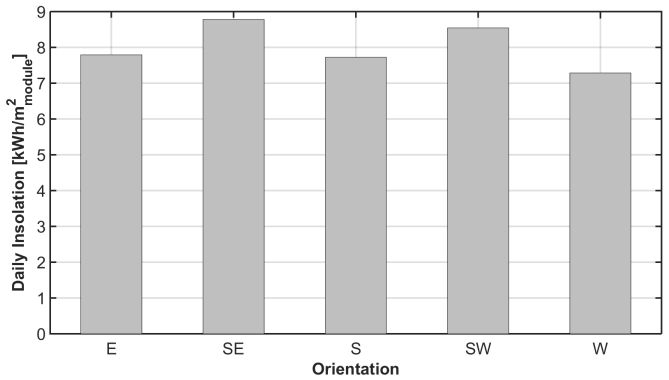

Figure 12: Daily insolation on the PV module of ZigZagSolar™ BIPV facade in Eindhoven on a summer day as a function of facade orientation.

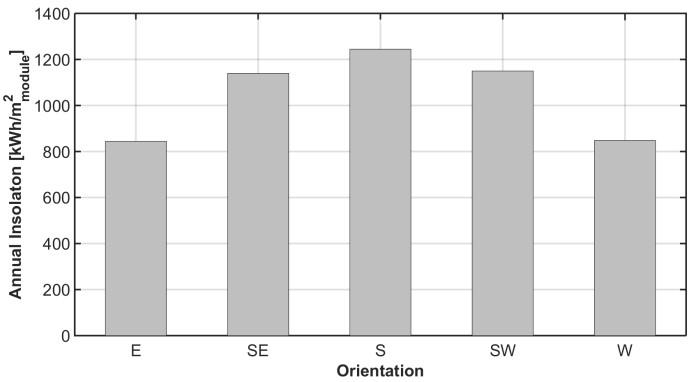

Figure 13: Annual insolation on the PV module of ZigZagSolar™ BIPV facade in Eindhoven as a function of facade orientation.

shows that although the South orientation is not optimum for a sunny summer day (see section 4.2), it is still the best orientation, at least for the city of Eindhoven, when considering one full year. Note that this analysis was done with a minimum of computational time. It only requires one single integration of the product of sensitivity and integral sky map. The results for the different orientations are obtained by simply repeating this calculation with a rotated sensitivity map.

5. Discussion

The reason that this irradiance model is computationally efficient is because it decouples the information regarding the weather conditions (stored in the sky map) from the information regarding geometry and optical properties of the PV module and its surroundings (stored in the sensitivity map). This means that once the sensitivity map is generated for a particular PV system it can be combined with any sky map to quickly predict the irradiance on the PV module for any location and time. When the PV system is redesigned, the sensitivity map can be recalculated and the irradiance model can be used to quickly test whether this will increase the incident irradiance. The sensitivity map can even be used as a guide when optimizing a PV system for a particular location as the maximum irradiance is achieved when there is maximum overlap between the bright parts in sky and sensitivity maps.

6. Conclusion

In this paper a flexible irradiance model based on the combination of sky map and sensitivity map was presented. This model was validated experimentally for the ZigZagSolar™ BIPV facade that combines PV modules with mirror reflectors. The model showed a very good agreement with the measured irradiance distribution and for most of the day the deviation was less than 10%. This irradiance model was then used to predict the annual insolation for the city of Eindhoven for different facade orientations. This showed that for this mirror reflector with an angle of 25°, the Southeast or Southwest oriented system outperforms the South oriented system for a sunny summer day. However for a full year, the South orientation is still the optimum.

7. Acknowledgment

The authors would like to thank Roel Loonen of TU Eindhoven for useful discussions and Simon Thiele of SEAC for assistance with the measurements. The work is supported by Netherlands Enterprise Agency (RVO) and the Dutch Topteam Energy via the project: ZonneGEVEL with grant number TEZG114003.

References

[1] PVsyst, `http://www.pvsyst.com/`, accessed: 2016-09-24.

[2] Meteonorm, `http://www.meteonorm.com/`, accessed: 2016-09-24.

[3] D. Reindl, W. Beckman, J. Duffie, Evaluation of hourly tilted surface radiation models, Solar Energy 45 (1) (1990) 9 – 17. `doi:http://dx.doi.org/10.1016/0038-092X(90)90061-G`. URL `http://www.sciencedirect.com/science/article/pii/0038092X9090061G`

[4] R. M. E. Valckenborg, W. van der Wall, W. Folkerts, J. L. M. Hensen, A. de Vries, ZigZag structure in facade optimizes PV yield while aesthetics are preserved, 32nd EU PVSEC, 2016, pp. 2486–2491.

[5] T. Kolås, A. K. Royset, Solar reflection losses in cover glass with asymmetric v-grooves for vertical south oriented pv-module, in: Optical Nanostructures and Advanced Materials for Photovoltaics, Optical Society of America, 2012, pp. JT3A–5.

[6] P. Tregenza, I. Waters, Daylight coefficients, Lighting Research and Technology 15 (2) (1983) 65–71.

[7] D. Bourgeois, C. Reinhart, G. Ward, Standard daylight coefficient model for dynamic daylighting simulations, Building Research & Information 36 (1) (2008) 68–82.

[8] C. F. Reinhart, O. Walkenhorst, Validation of dynamic radiance-based daylight simulations for a test office with external blinds, Energy and buildings 33 (7) (2001) 683–697.

[9] R. Perez, R. Seals, J. Michalsky, All -weather model for sky luminance distribution -preliminary configuration and validation, Solar energy 50 (3) (1993) 235–245.

[10] LightTools, https://optics.synopsys.com/lighttools/, accessed: 2016-09-24.
[11] ZigZagSolar, http://zigzagsolar.com/, accessed: 2016-09-24.
[12] R. M. E. Valckenborg, J. L. M. Hensen, W. Folkerts, A. de Vries, Characterization of BIPV(T) applications in research facility SolarBEAT, 31st EU PVSEC, 2015, pp. 2911 – 2916.
[13] A. Smets, K. Jäger, O. Isabella, R. van Swaaij, M. Zeman, Solar Energy, the physics and engineering of photovoltaic conversion technologies and systems, UIT Cambridge, 2016, p. 271-274.